Differential deposition technique for figure corrections in grazing incidence X-ray optics

Kiranmayee Kilaru[1], Brian D. Ramsey[2], Mikhail V. Gubarev[2]

[1]University of Alabama in Huntsville, Huntsville, AL, 35899

[2]NASA Marshall Space Flight Center (MSFC), Huntsville, AL, 35812

ABSTRACT

A differential deposition technique is being developed to correct the low- and mid-spatial-frequency deviations in the axial figure profile of Wolter type grazing incidence X-ray optics. These deviations arise due to various factors in the fabrication process and they degrade the performance of the optics by limiting the achievable angular resolution. In the differential deposition technique, material of varying thickness is selectively deposited along the length of the optic to minimize these deviations, thereby improving the overall figure.

High resolution focusing optics being developed at MSFC for small animal radionuclide imaging are being coated to test the differential deposition technique. The required spatial resolution for these optics is 100 μm. This base resolution is achievable with the regular electroform-nickel-replication fabrication technique used at MSFC. However, by improving the figure quality of the optics through differential deposition, we aim at significantly improving the resolution beyond this value.

Keywords: X-ray optics, Differential deposition

1. BACKGROUND

X-rays are reflected off the smooth surfaces when incident at graze angles less than the critical angle. This phenomenon, called the total external reflection, is utilized to reflect the X-rays for imaging. Wolter optical designs developed by Hans Wolter in 1952 [1], uses a combination of hyperbolic parabolic and/or elliptical mirrors to perform X-ray imaging. These optical designs have been used in optics of astronomical telescopes to observe cosmic sources emitting high energy radiation [2].

Fabrication of Wolter configuration X-ray optics is done at MSFC using the Electroform Nickel Replication (ENR) Technique [3]. In this technique super polished Aluminum mandrels having desired surface profile are used to electroform NiCo shells, which are later separated by utilizing the difference in thermal expansion coefficient of two metals. Shells of decreasing diameter are nested within one another to form an imaging X-ray optics. Several factors in the fabrication process, such as deviations in the surface profile of mandrel, stress during the electroforming process cause deviations in the surface profile of the shell from the desired profile which can lead to poor imaging quality of the optics resulting in the degradation of achievable resolution.

The purpose of the study is to investigate a differential deposition technique which can minimize the undesired deviations in the axial figure profile of the shell, thereby improving the imaging quality of Wolter type grazing incidence X-ray optics.

2. INTRODUCTION

The differential deposition technique involves axially depositing material of varying thickness along the length of the shell. Thicker coating is deposited at positions of higher deviation and thinner coating at low deviation positions. RF sputtering is used to perform this deposition. The target metal rod (from the material is sputtered), a mask and the shell to be corrected are concentrically positioned over one another as shown in Figure 1. The mask has a slit of definite width to limit the spatial extent of deposition. Slit-width is chosen to correct specific frequency deviations. The shell rotates over the mask and is translated linearly over the slit of the mask with a variable velocity.

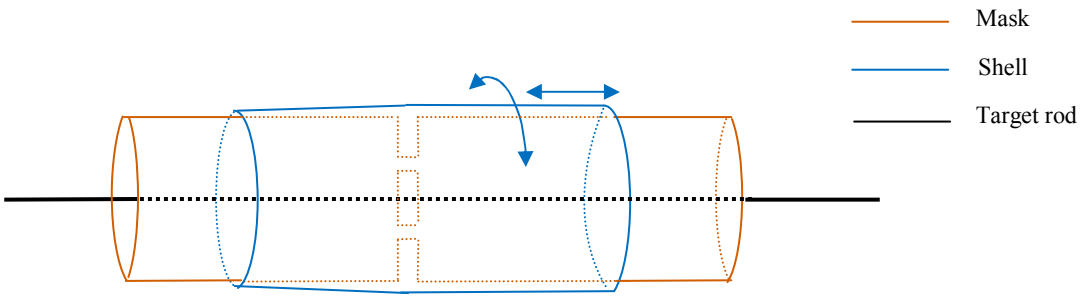

Figure 1: Target rod, mask and slit positioned concentrically over one another. Shell is rotated over the mask while it is translated linearly with variable velocity.

The complete system is placed in the vacuum chamber filled with inert gas at low pressure. An AC bias of high frequency, typically 13.56 MHZ is applied to the target surface. When the target is negatively charged any free electron present in the chamber accelerates away from the target, hits the inert gas atom and creates a positively charged inert gas ion by knocking off the outer shell electron of the atom. The effective negative bias voltage of the target causes the positively charged ion to hit the target with high energy, resulting in sputtering of atoms from the target surface. Sputtered target material passes through the slit and gets deposited on the shell. By controlling the translation velocity of the shell, material of varying thickness gets deposited on the shell. Translation velocity is inversely proportional to the deposition thickness required. The amplitude of profile deviations on the shell in terms of height feeds as input to variable velocity of the shell in terms of time. Figure 2 shows cross sectional depiction of desired profile and deviations in the measured profile that get minimized after the differential deposition corrections. The deviations are exaggerated for depiction purpose.

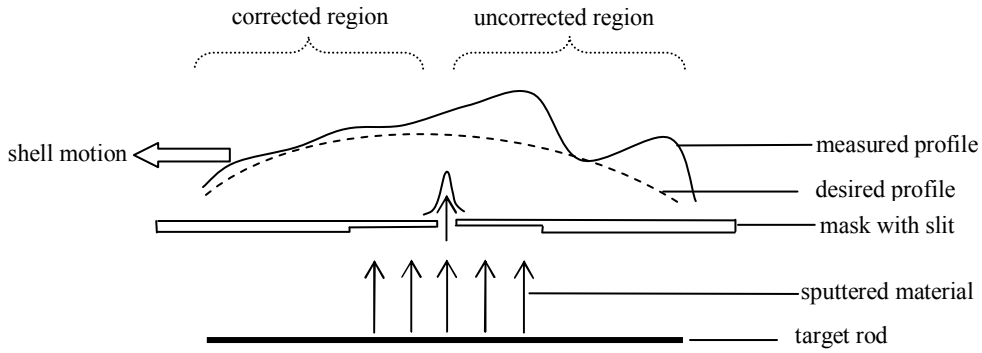

Figure2: Sputtered target material passes through the slit and gets deposited on the shell.

3. APPLICATION

Differential deposition technique will be implemented as a proof of concept on small animal radionuclide imaging focusing X-ray optics. This optics is being fabricated at MSFC and will be used for noninvasive radionuclide

imaging to perform functional and metabolic assessment in small animals. This multilayer coated optics is designed to focus either the 18 keV photons emitted by ^{99m}Tc or the 27 keV photons emitted by ^{125}I. The optics used a combination of confocal hyperbolic and elliptical segments to perform on-axis imaging. Figure 3 shows the picture of the shells developed at MSFC. The shell has hyperbolic profile on one half of the lateral segment and elliptical profile on other half. Figure 4 gives cross sectional view of the optical layout with object located at the right focal point of the hyperbola and image at the right focal point of the ellipse.

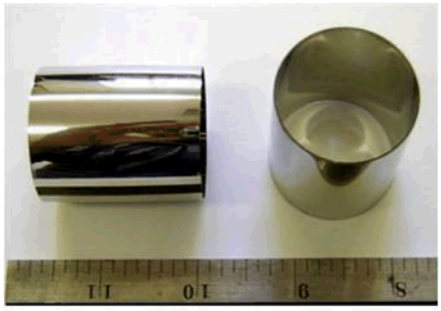

Figure 3: Small animal radionuclide imaging focusing X-ray optics

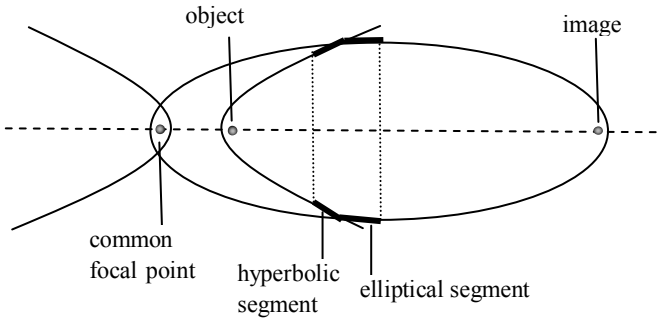

Figure 4: Confocal hyperbola and ellipse geometry

Starting at the object, X-rays that hit hyperbolic segment at graze angle less than critical angle get reflected off to the elliptical segment and then to the image location. Any deviations in the surface profile of the hyperbolic and elliptical segments degrade the imaging quality of the optics. The targeted spatial resolution with this optics is 100 μm which is believed to be achieved with the regular Electroform Nickel Replication process. We aim at improving the performance of optics beyond this targeted value using the differential deposition technique.

4. SIMULATIONS/EXPERIMENTS

A mathematica program is developed to perform 2D ray tracing for the X-ray optics with surface profile deviations. This program is used to simulate the performance of the optics before and after the figure corrections with differential deposition. Also simulations were done to develop a strategy for the correction of surface deviations with the differential deposition technique. Plot in Figure 5 shows the simulated and measured profile of the beam of sputtered material that gets through a 5mm slit mask and deposits on the shell. The profile depends on the slit-width, distance between the mask and shell and the mask thickness. The Full width half maximum of the profile increases with increasing distance between the mask and shell. Finer beam profiles are often needed for finer deviation corrections, so minimum possible mask to shell distance is maintained which determines the radius of the mask. Increased mask thickness results in decreased deposition rate with less sputtered material reaching the shell. This leads to the increase of the deposition time when correcting a shell. Therefore, thinner mask is chosen to obtain higher deposition rates. The mask to shell distance of 0.2 mm and the shell thickness of 0.3 mm are used for profile shown in Figure5. Figure 6 shows series of steps followed in the simulations of shell correction strategy. For a given desired coating profile that is needed to correct a shell, the sputtered beam is scanned along with definite step size and with amplitude varying according to the desired coating profile. The ratio of the amplitudes of the added thickness of the scanned beam and the desired coating thickness along with the deposition rate

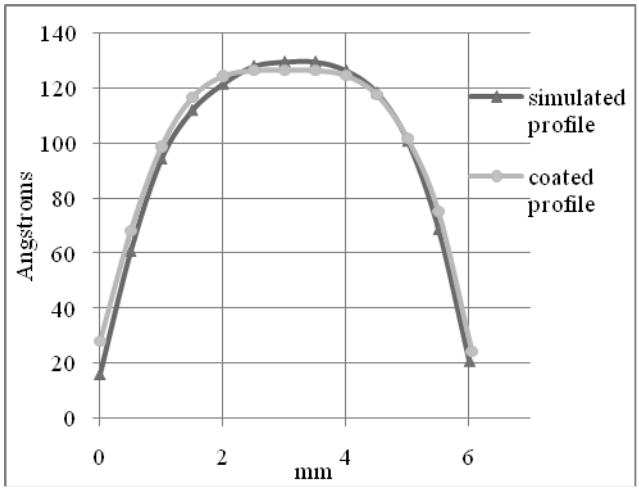

Figure 5: Simulated and coated sputtered beam profile for 5mm mask

dictates the dwell time at each position. This position vs dwell time data obtained from the simulations is used as an input for the translation velocity of the shell.

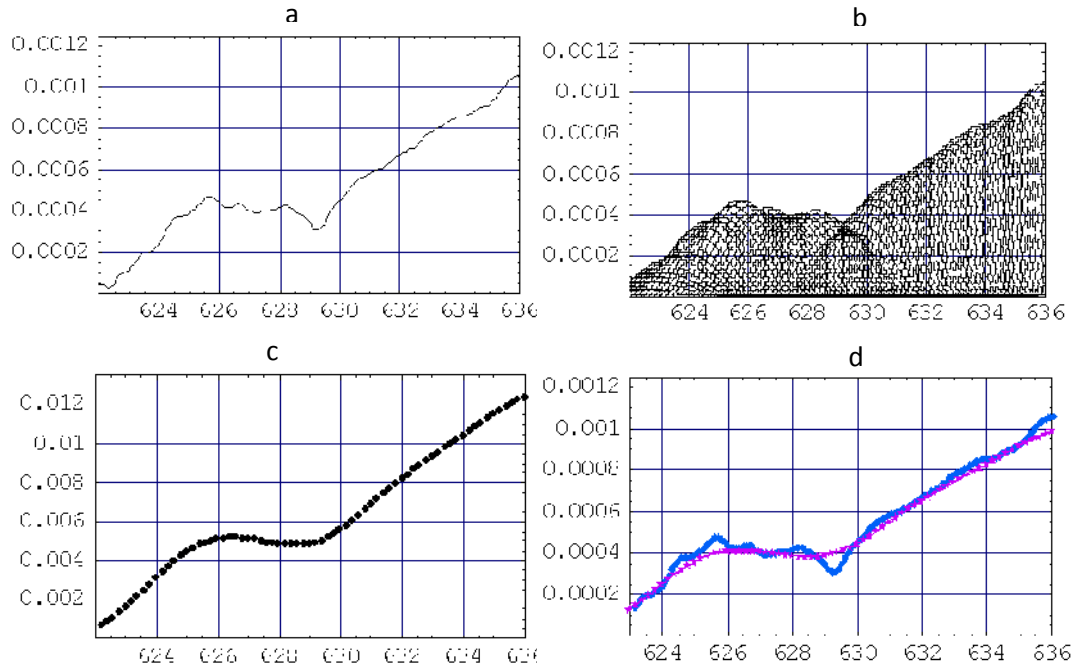

Figure 6: a. desired coating profile, b. sputtered beam profiles scanned along the desired profile, c. added profile of the scanned beam, d. ratioed added profile compared to desired profile

For the figure correction on a shell, deposition is done in a series of steps starting with coarser deviation corrections using a broader slit-width, followed by a series of finer deviation corrections using narrower slits. Selection of slit-width depends on the spatial frequency of the deviation to be corrected. Figure 7 is the simulation result showing the comparison of profiles on hyperbola and ellipse before and after the differential deposition correction done with a series of 5mm, 2mm and 1mm slit sizes.

Figure 8 gives picture of the vacuum chamber used to perform the differential deposition. The vacuum chamber has the rotational and translation stages to rotate and translate the shell over the mask. These stages are calibrated to perform precise and accurate motion. Various mask configurations were tried in order to obtain stable and symmetric plasma around the slit. Target rod has to be centered perfectly with respect to mask in order to obtain symmetric plasma. Any deviations in the centering leads to asymmetric deposition rate around the slit. The shell is rotated over the slit to address for any such asymmetries. Also, the mask is bored out, as shown in the Figure 2, in the center region near the slit to define the region of plasma formation and so the region of sputtering inside the mask. This helps in avoiding the large angle sputtering which lead to poor coating quality. Figure 6 shows a photograph of the mask that will be used to perform deposition on the X-ray optics.

Background experiments have been done to determine the tradeoff between experimental variables such as the deposition material, power setting of the RF sputter deposition, the inert gas used in the vacuum chamber and pressure of the inert gas. The goal is to determine the optimum setting that has higher deposition rate, good surface quality with of the coating and good adhesion with low stress. Coatings were done on 2mm thick D263 glass which has roughness levels in the range of 2-4 A^0. Roughness of the coatings was measured on these samples. Coatings were also done on NiCo metal samples to test for the adhesion.

Platinum, Tungsten, Nickel material coatings were tried with Xenon and Argon inert gases. Various combinations of forward power of the target and pressure of the inert gas were tried. Table 1 gives the roughness and deposition rate values for a certain combination of these variables. Some of coatings for example Tungten-Argon at 90-30 had high stress and were peeled off having poor surface quality. Nickel has higher adhesion values and Nickel-Xenon has higher deposition rates than Nickel-Argon. Also, this combination has higher roughness values for increased pressure. The chosen setting to perform deposition on the X-ray optics is Nickel with Xenon at 75 W forward power and 15mTorr Xenon gas pressure. This setting has the estimated deposition rate of 0.29 A^0/sec, 1.915 rms roughness and 100% adhesion when tested with scotch tape for 5000A^0 coating thickness. Thickness measurements were made using a TENCOR step profilometer and roughness measurements were done using WYKO.

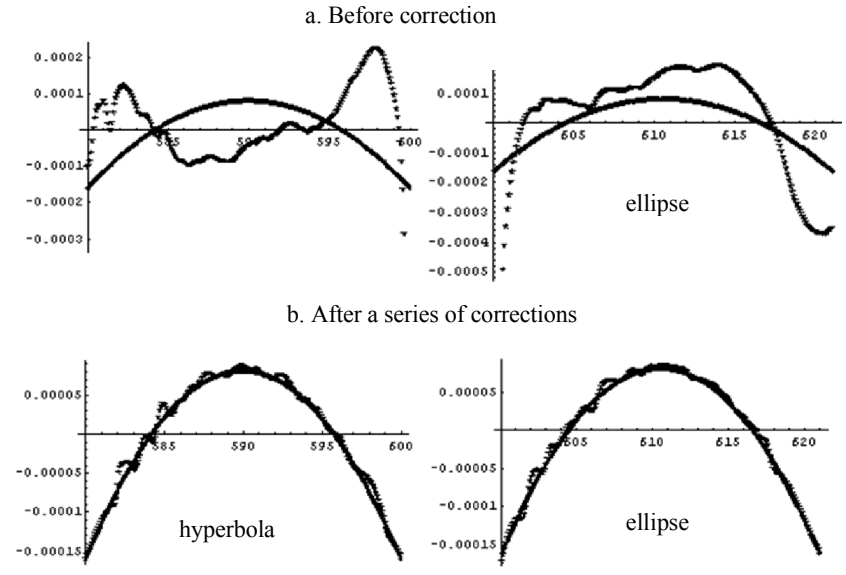

Figure 6: a. hyperbola and ellipse profiles before correction; b. profiles after a series of corrections.

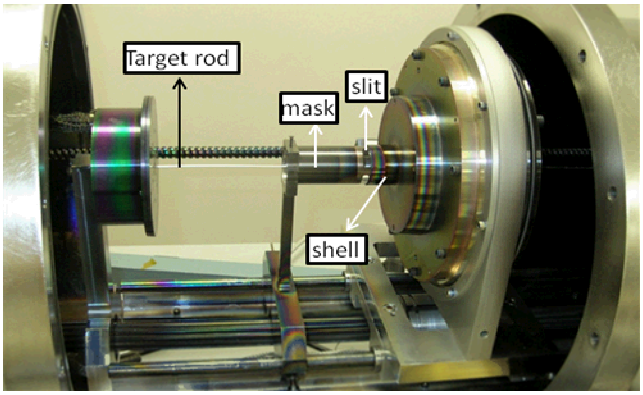

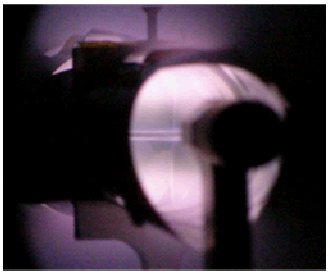

RF Sputter deposition - Xenon plasma

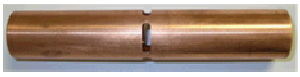

Mask configuration

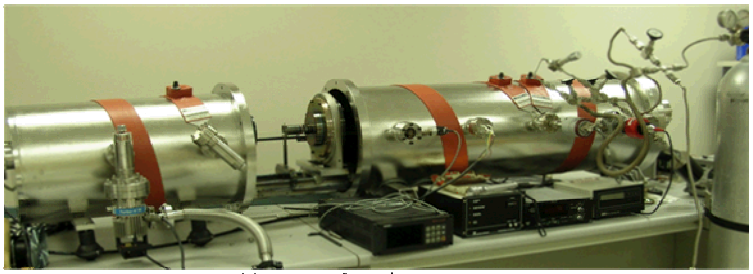

Vacuum chamber

Figure 7: Pictures of experimental set up, vacuum chamber, Xenon plasma and mask configuration.

Platinum-Xenon				Platinum-Argon			
power	pressure	roughness	deposition rate	power	pressure	roughness	deposition rate
75	15	1.950	0.130	75	15	2.060	0.140
90	15	2.043	0.230	90	15	1.933	0.190
75	30	1.895	0.170	75	30	1.868	0.160
90	30	1.810	0.250	90	30	2.083	0.220
Nickel-Xenon				Nickel-Argon			
power	pressure	roughness	deposition rate	power	pressure	roughness	deposition rate
75	**15**	**1.915**	**0.290**	75	15	1.995	0.180
90	15	2.070	0.360	90	15	1.778	0.240
75	30	3.093	0.240	75	30	2.260	0.220
90	30	3.630	0.310	90	30	2.210	0.290
Tungsten-Xenon				Tungsten-Argon			
power	pressure	roughness	deposition rate	power	pressure	roughness	deposition rate
75	15	1.965	0.300	75	15	1.900	0.120
75	30	1.805	0.290	75	30	2.125	0.290
90	30	1.993	0.370	90	30	-	-
75	50	2.075	0.290	75	50	1.998	0.310
90	50	2.423	0.370	90	50	1.868	0.370
Units: power – Watts, Pressure – mTorr, Roughness – A ^{0} rms, deposition rate – A ^{0}/sec							

Table 1: Roughness and deposition rates of the coating for certain combination of experimental variables.

Initial trials of differential deposition were done on glass. Figure 8 shows a picture of differential deposition done on glass and the plot depicts comparison between the desired and coated profiles. Trials are in progress to perform differential deposition on the small animal radionuclide imaging shells.

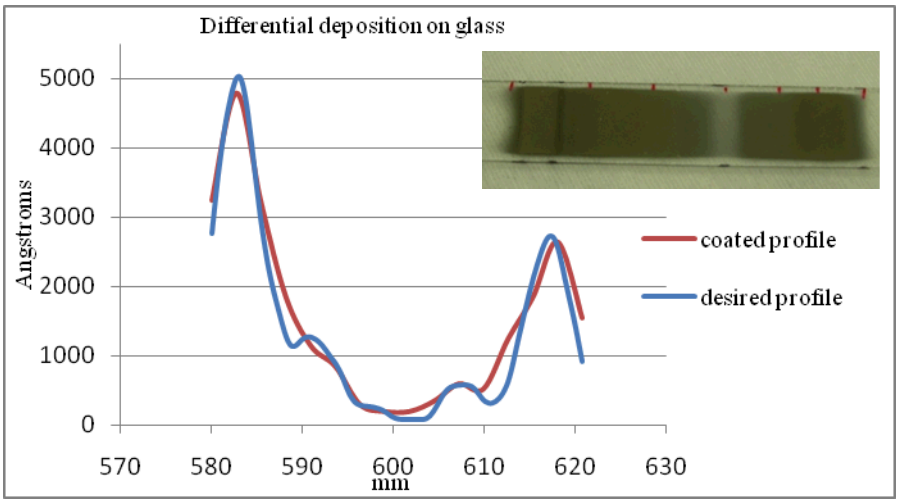

Figure 8: Differential deposition on glass

5. ONGOING WORK

To obtain a performance better than 10 arc secs with small animal radionuclide imaging, deviations up to the level of 500 A^0 have to be corrected. This can be done only if the surface profiles can be measured accurately with reproducibility better than 100 A^0. The profile of X-ray optics is measured using a contact profilometer with the optics held on a specially designed mount shown in the figure 7 below.

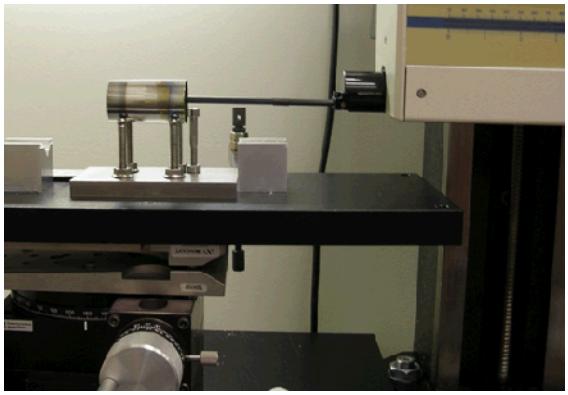

The profile measurements taken in such a way have reproducibility of about +/-1000 A^0, which makes it difficult to determine accurately the actual profile on the optics. Efforts are in progress to overcome this problem, one way of which is averaging several measured data sets taken repeatedly along the same position. This assumes that the error introduced is random and that it gets nullified on averaging. The averaging technique improved the reproducibility to about +/- 200 A^0. Figure 7 is the plot that shows a comparison of the difference between 2 data sets and the difference between averages of 18 data sets.

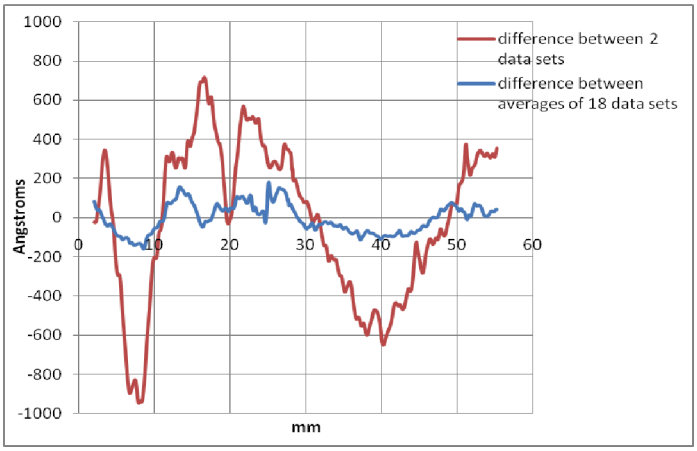

Experiments are underway to minimize the surface deviations in small animal radionuclide focusing X-ray optics using this differential deposition technique. Figure 8 shows the photograph of the X-ray test up, built in house to test the performance of this optics. This test setup uses microfocus X-ray source with 20 µm source size. A voltage of 12 kV and current of 0.3 mA are used while operating microfocus X-ray source. Silicon X-ray detector is used to detect the radiation. Image resolution is measured using laser cut Tungsten pinholes. Small animal imaging optics has the total optical path length of about 3m. The cutoff energy seen by the optics with no multilayer coatings is about 7 keV. At

such low energies X-rays get attenuated in air before reaching the detector. A tube filled with Helium is used along the optical length to reduce the signal attenuation. The detector is mounted on a 2-axis translation stage and the optics on a translational and 2-axis rotational stage for alignment. This test set up will be used to test the imaging quality of the optics before and after performing the differential deposition.

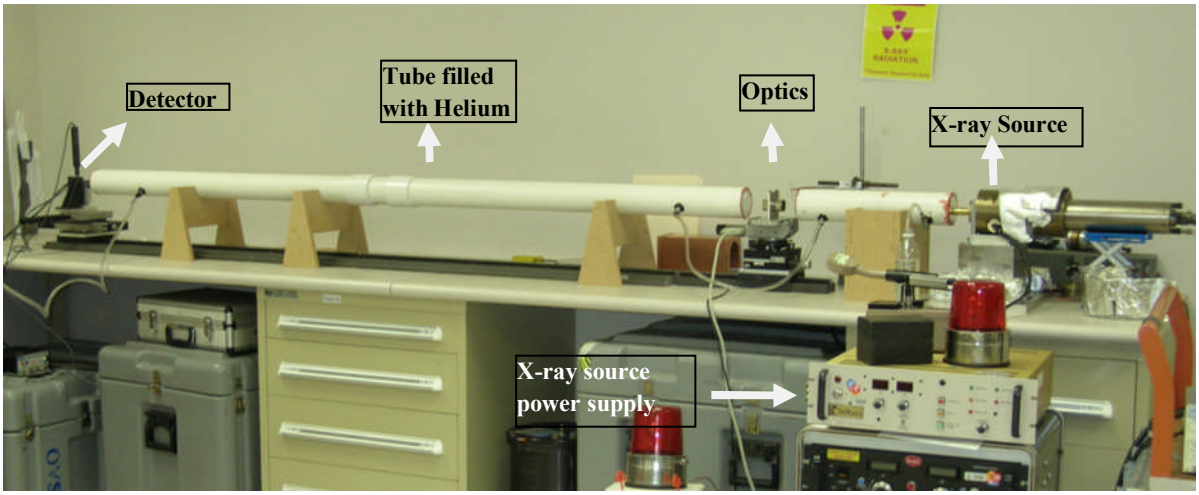

Figure 8: Experimental set up to test the performance of small animal radionuclide imaging X-ray optics

CONCLUSIONS

A differential deposition technique is under investigation which can be used to minimize the surface deviations in Wolter type X-ray optics. Background experiments to determine the tradeoff between several experimental variable have been completed and experiments are in progress to perform the differential deposition on the X-ray optics. As a proof of concept this technique is being investigated on small animal radionuclide imaging X-ray optics. Also an X-ray test setup has been developed to test the performance of the optics before and after coating.

REFERENCES

1) Wolter, H., "Spiegelsysteme streifenden Einfalls als abbildende Optiken fur Rontgenstrahlen," Ann Physik, 10, pp. 94-114 (1952).
2) Giacconi R., Harmon N. F., Lacey R. F., Szilagyi Z., "Aplanatic telescope for soft x-rays", J Opt Sco Amer, 55, pp. 345-347 (1965).
3) Ramsey, B., D., *et al.*, "The development of hard X-ray optics at MSFC," Proc SPIE 5168, pp. 129-135 (2004).
4) Soichiro Handa, Hidekazu Mimura, Hirokatsu Yumoto, Takashi Kimura, Satoshi Matsuyama, Yasuhisa Sano, Kazuto Yamauchi, "Highly accurate differential deposition for X-ray reflective optics", Surface and Interface Analysis, 40, pp.1019-1022 (2008).
5) Pivovaroff, M. J., Barber, W. B., Christensen, F. E., Craig, W. W., Decker, T., Epstein, M., Funk, T., Hailey, C. J., Hasegawa, B. H., Hill, R., Jernigan, J. G., Taylor, C., Ziock, K., "Small animal radionuclide imaging with focusing gamma-ray optics," Proc SPIE, 5199, pp. 147-161 (2004).
6) Pivovaroff, M. J., Funk, T., Barber, W. C., Ramsey, B. D., Hasegawa, B. H., "Progress of focusing x-ray and gamma-ray optics for small animal imaging," Proc SPIE, 5923, pp. 65-78 (2005).